coatings

MDPI

*Supplementary Information*

# Enhanced Electrocatalytic $CO_2$ Reduction of Bismuth Nanosheets with Introducing Surface Bismuth Subcarbonate

**Shiyuan Liu [1], Botao Hu [1], Junkai Zhao [1,2], Wenjun Jiang [1], Deqiang Feng [1], Ce Zhang [1,*] and Wei Yao [1,*]**

[1] Qian Xuesen Laboratory of Space Technology, China Academy of Space Technology (CAST), Beijing, 100094, China; liushiyuanchn@yeah.net (S.L.); hubotao@qxslab.cn (B.H.); 202031150009@mail.bnu.edu.cn (J.Z.); jiangwenjun@qxslab.cn (W.J.); fengdeqiang@qxslab.cn (D.F.)

[2] Beijing Key Laboratory of Energy Conversion and Storage Materials, College of Chemistry, Beijing Normal University, Beijing 100875, China

* Correspondence: zhangce@qxslab.cn (C.Z.); yaowei@qxslab.cn (W.Y.)

**Evaluation of $CO_2$RR performance**

The gas Faradaic efficiency (FE) was calculated based on the differential forms of the Faradaic formula. The molar flow of gas from the flow-cell reactor was calculated using the concentration of species m measured by GC ($x_g$, (mol mol$^{-1}$)) and the $CO_2$ flow rate ($f_{CO2}$ (mol s$^{-1}$)). Considering the low concentration of gas production and that the outlet is connected to the air, the molar ratio ($x_g$) can be replaced by partial pressure directly. So, the $FE_m$ is the percentage of the partial current in the total current ($i_{tot}$, (A)):

$$FE_g\ (\%) = i_g/i_{tot} \times 100\% = 96485 \times x_g \times f_{CO2} \times z_g/i_{tot} \times 100\% \quad (1)$$

The FE of the formate ion in liquid was calculated based on the concentration ($c_l$, mol L$^{-1}$) detected by High Performance Liquid Chromatography (HPLC).

$$FE_l\ (\%) = q_l/q_{tot} = 96485 \times c_l \times V \times z_l/q_{tot} \times 100\% \quad (2)$$

V was the volume of the cathode electrolyte and $q_{tot}$ was the total Coulomb electricity.

The long-term electrocatalytic $CO_2$ reduction reaction measurements were conducted in a three-electrode flow-cell reactor. The catholyte and anolyte were both 0.5 M $KHCO_3$ and were separated by an anion exchange membrane with a flow rate of 20 sccm. Figure S10 is the experimental equipment placement. A gas chromatography (GC, Shimadzu GC-2014C) set-up was employed for the gas analysis. A half a milliliter of product was injected into the GC to analyze the gas species and concentration on the appointed chronoamperometry. Meanwhile, the liquid was collected after each chronoamperometry.

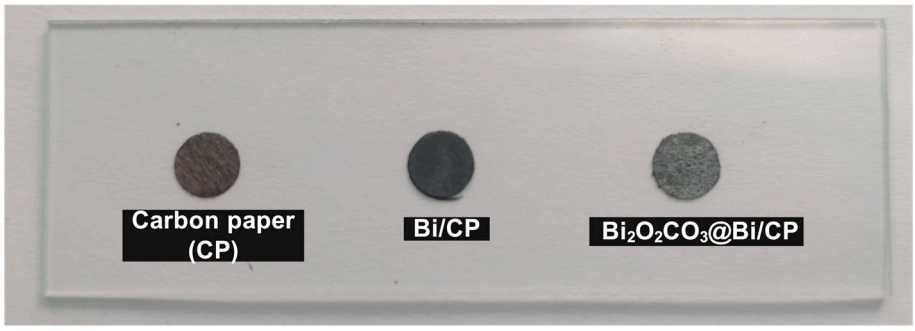


**Figure S1.** The sample photo of original carbon paper, dendrite Bi/CP, and $Bi_2O_2CO_3$@Bi/CP.

As the image shows, the surface morphology transformation can be observed easily. The $Bi_2O_2CO_3$@Bi/CP sample appeared as a white color. In fact, the transformation degree is related to the exposure time for the Bi nanosheets, but is hard for the Bi dendrite.

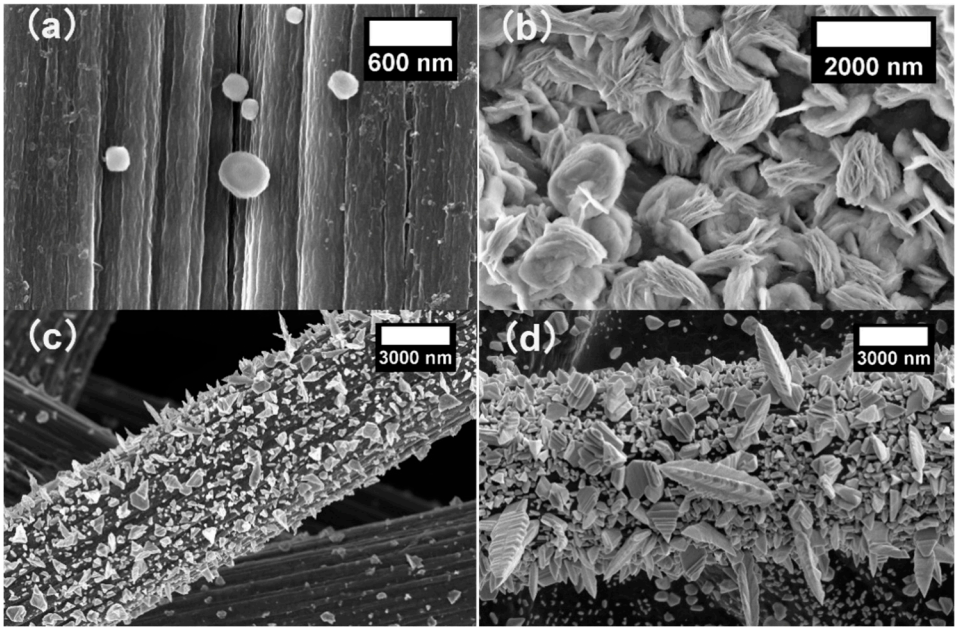


**Figure S2.** SEM images of samples on different pulse current: (**a**) 0.4 mA $cm^{-2}$, (**b**) 0.8 mA $cm^{-2}$, (**c**) 1.2 mA $cm^{-2}$, and (**d**) 1.6 mA $cm^{-2}$.

Under the different pulse current conditions, the Bi/CP samples' crystal morphologies are distinct. A scattered Bi nucleus was grown on the carbon paper under 0.4 mA $cm^{-2}$. In contrast, the Bi metal was grown into a bulk-structured form at 1.2 mA $cm^{-2}$ and with a larger current.

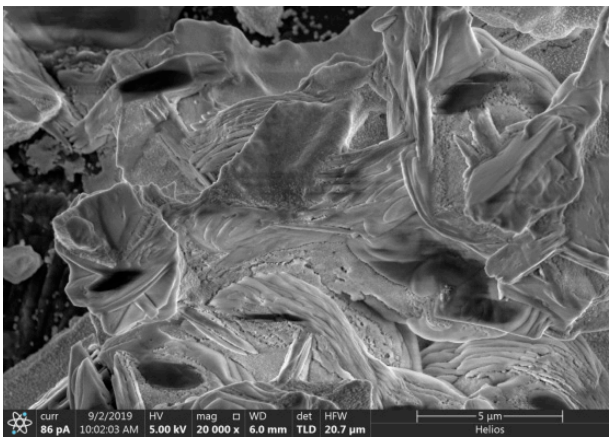

**Figure S3.** SEM image of electrode at 90 min electrodeposition with a current density of 0.8 mA $cm^{-2}$.

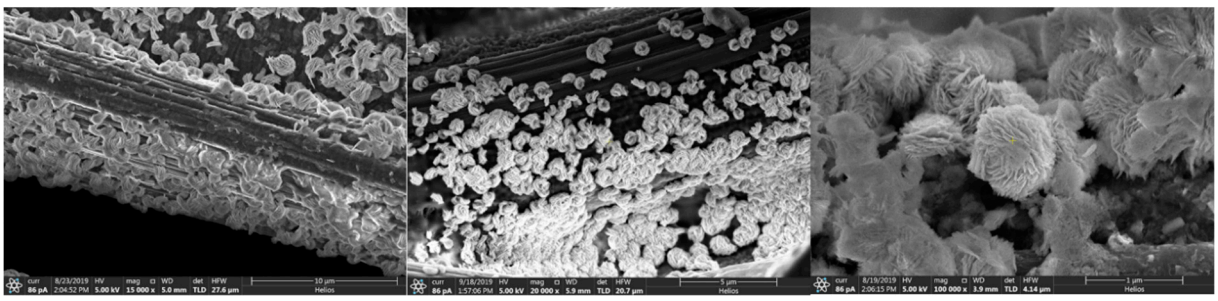

**Figure S4.** SEM photographs at different magnifications.

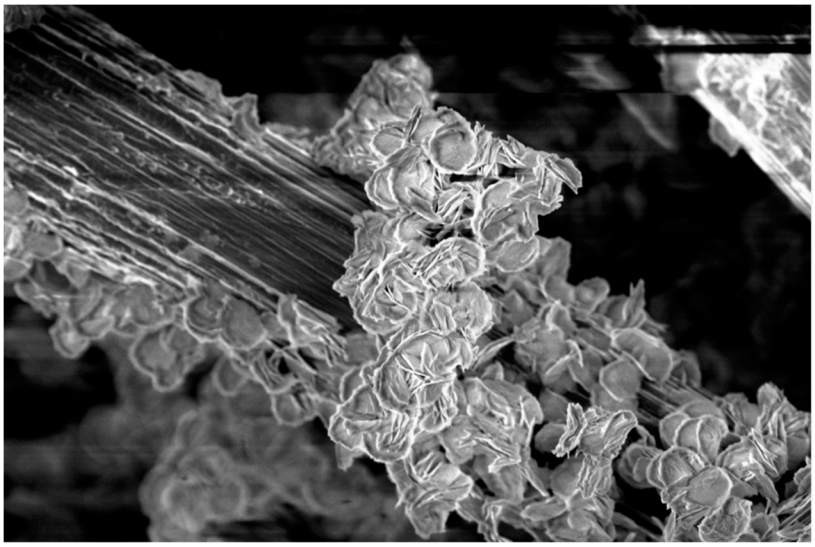

**Figure S5.** SEM characterizations of a flower-like Bi sample exposed in air for a long time (>60 h).

After a long-term air exposure, $CO_2$ and $O_2$ reacted with the Bi nanosheets and formed $Bi_2O_2CO_3$.

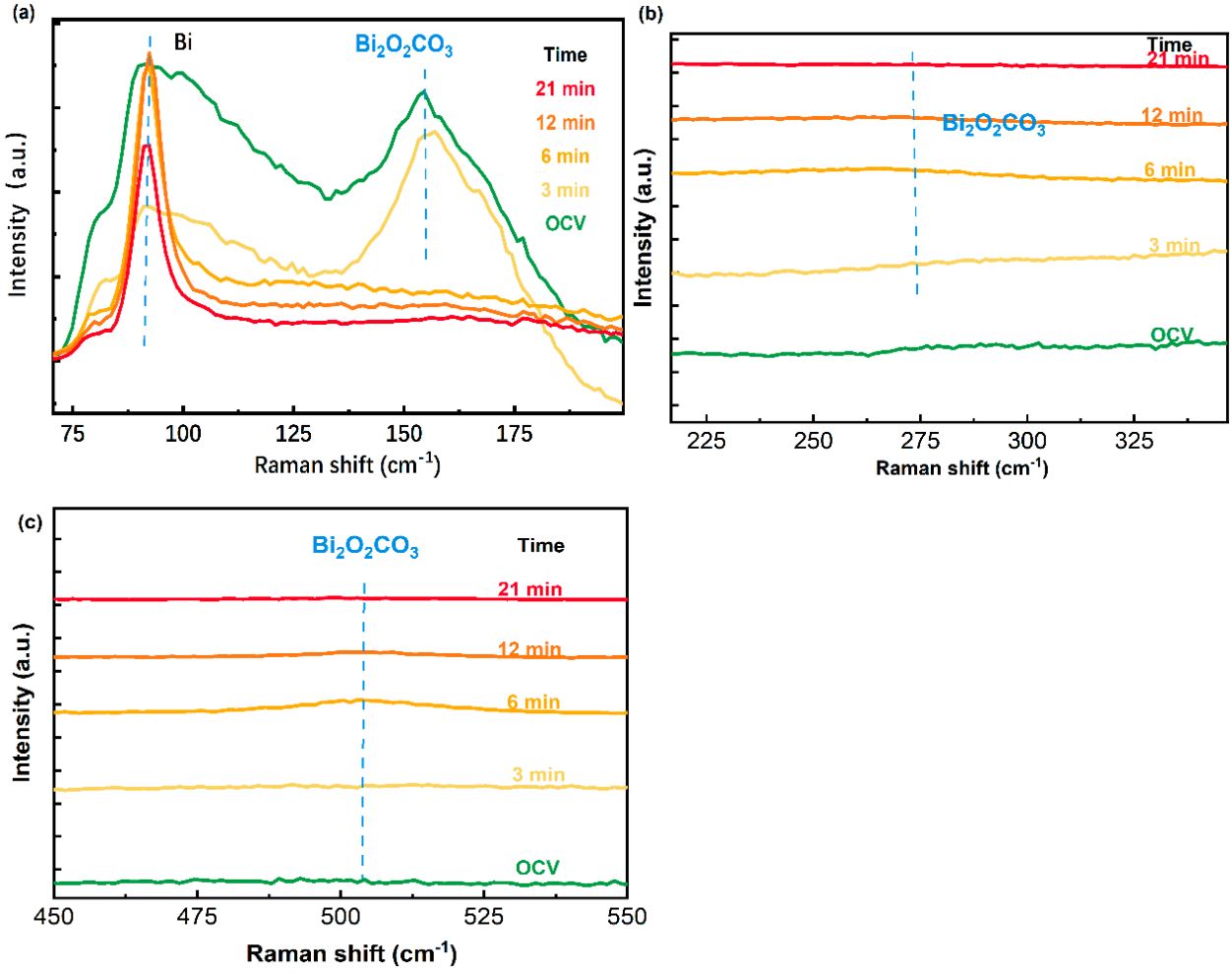


**Figure S6.** The particular Raman spectra of $Bi_2O_2CO_3$@Bi/CP: (**a**) the Bi–Bi bond peak and Bi–O bond peak; (**b**) the broad external vibration peaks on $Bi_2O_2CO_3$; and (**c**) the Bi=O bond peak.

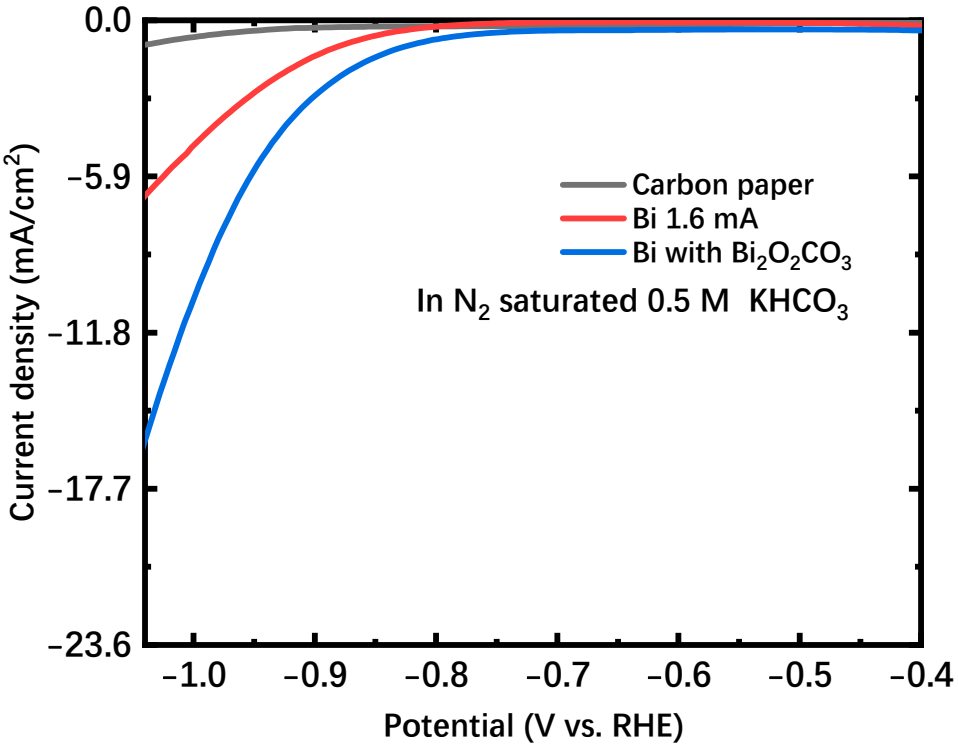


**Figure S7.** LSV curves of Carbon paper, Bi/CP, and $Bi_2O_2CO_3$@Bi/CP in the $N_2$ saturated 0.5 M $KHCO_3$.

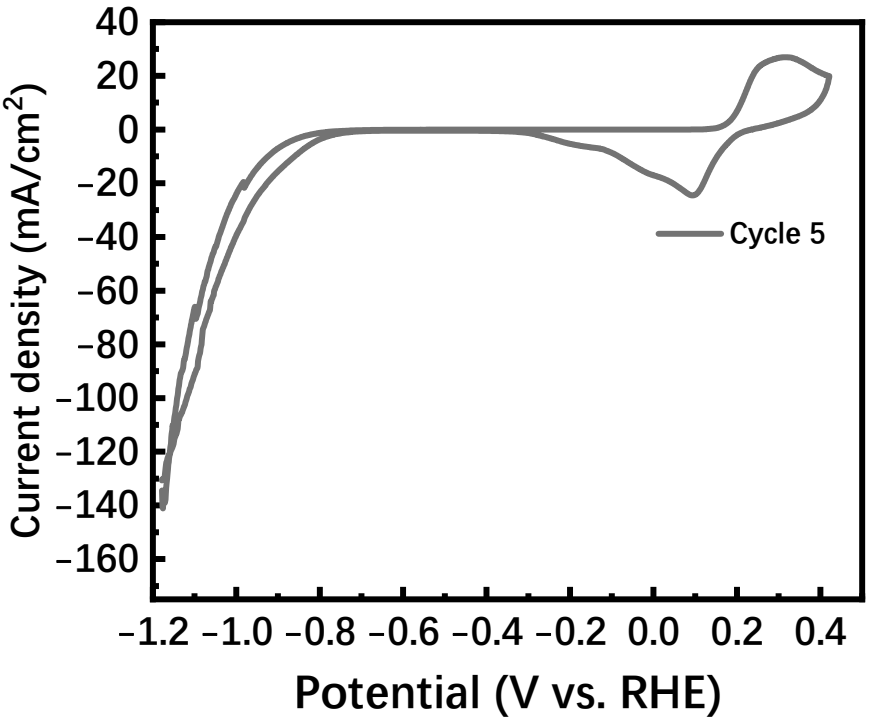


**Figure S8.** The typical CV curve of a pristine $Bi_2O_2CO_3$@Bi/CP at scanning rate of 20 mV $s^{-1}$ from −1.2 to 0.4 V vs. RHE.

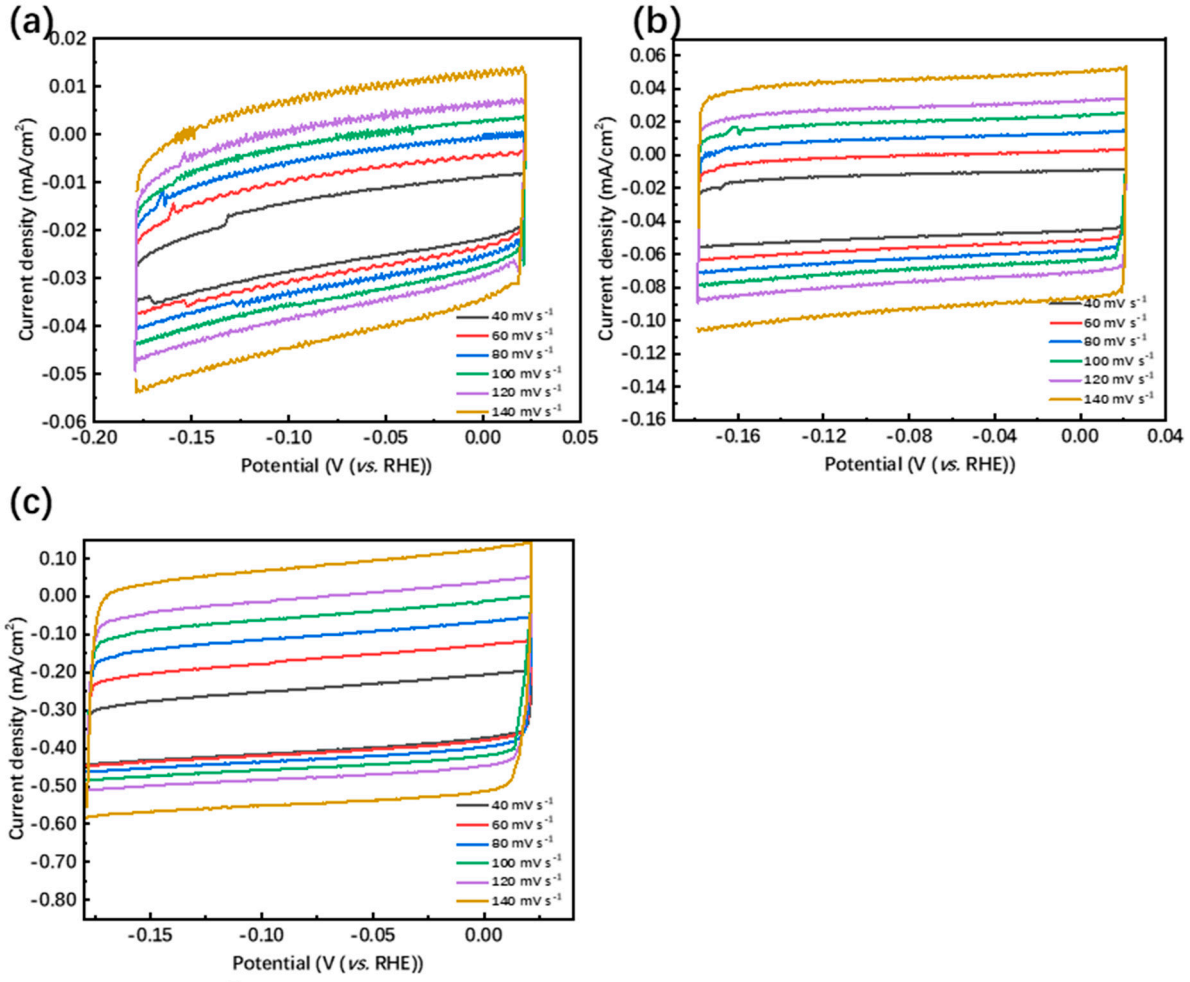


**Figure S9.** CV curves of different samples: (a) the CV curves result of original carbon paper; (b) the CV curves test of Bi/CP; (c) the CV curves of $Bi_2O_2CO_3$@Bi/CP.

For measuring the double-layer capacitance of ($C_{dl}$) of different samples, the cyclic voltammetry (CV) curves were recorded at a non-Faradaic region of the potential, which was between 0.0 to −0.2 V vs. RHE (0.5 M $KHCO_3$). The scan rates were 40 to 140 mV $s^{-1}$ with an interval of 20 mV $s^{-1}$. The $C_{dl}$ was estimated by plotting the $\Delta j = (j_a - j_c)$ at −0.1 V vs. RHE ($j_c$ and $j_a$ were the cathodic and anodic current densities, respectively).

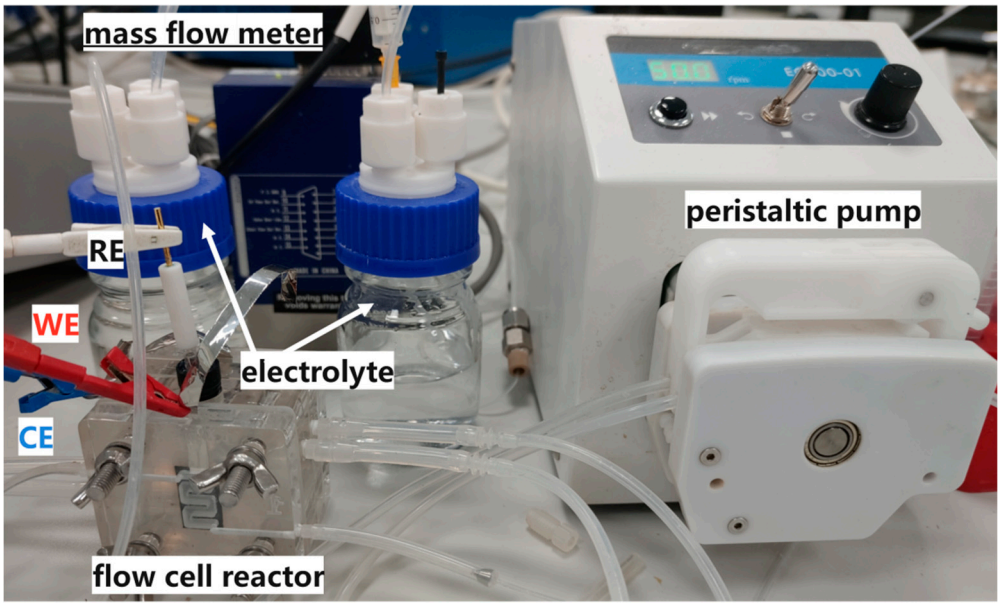


**Figure S10.** A flow cell rector for $CO_2RR$ with auxiliary equipment, including peristaltic pump, mass flow meter, resource gas, and electrochemical station.

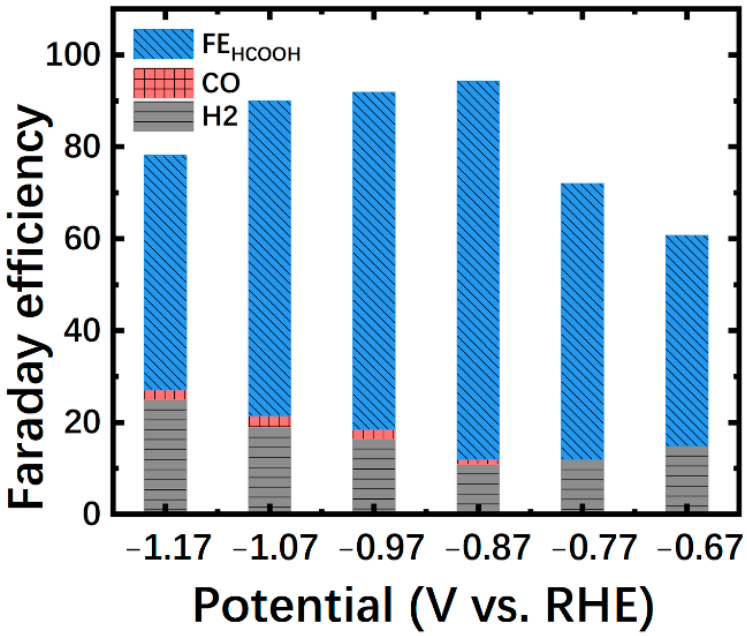


**Figure S11.** FE of $CO_2RR$ products at various potentials in $CO_2$-saturated 0.5 M $KHCO_3$ electrolytes on Bi/CP.